

Synthesis, Structure, and Magnetism of Np_2O_5

Tori Z. Forbes,[†] Peter C. Burns,^{*,†,‡} S. Skanthakumar,[‡] and L. Soderholm^{†,‡}

Department of Civil Engineering and Geological Sciences, University of Notre Dame, Notre Dame, Indiana 46556, and Chemistry Division, Argonne National Laboratory, Argonne, Illinois 60439

Received December 22, 2006; E-mail: pburns@nd.edu

Binary oxides, among the most fundamental of compounds, provide insight into an element's basic chemical properties, including oxidation state stabilities, coordination preferences, and bonding. This is particularly true for the 5f actinide series, which are known to be very oxophilic, with much of their chemistry demonstrated through the stability of oxide phases. Uranium exhibits the most structural variety in binary oxides, with numerous phases and solid solutions reported having U/O ratios between 1:2 and 1:3. An underlying reason for this variety is the stability of two prominent oxidation states, U(IV) and U(VI). Surprisingly, Pu, which has stable IV, V, and VI oxidation states in aqueous solution had, until recently, no binary oxide reported with a ratio greater than 1:2. The unexpected report of a PuO_{2+x} ^{1,2} phase has caused renewed interest in studying higher actinide oxides.

Np, with three stable oxidation states in solution, IV, V, and VI, has only two stable oxides, NpO_2 and Np_2O_5 , corresponding to stoichiometric Np(IV) and (V), respectively. Although the structure of the former compound is known, a detailed structural study of the latter has yet to be reported, in part because of the difficulty in synthesizing suitable single crystals. Reported routes to quality Np_2O_5 are limited to formation from high-temperature melts.³ Herein we report a low temperature, aqueous-based synthesis,⁴ and subsequent characterization, of phase-pure Np_2O_5 . The formation of this compound under such mild conditions is expected to have a significant impact on modeling the fate and transport of this radionuclide in the environment because Np(V) is usually considered highly soluble and unreactive. These results on Np_2O_5 will allow its further characterization in terms of thermodynamic stability and ultimately a reassessment of its role in the environmental chemistry of Np.

The structure of Np_2O_5 ⁵ contains three symmetrically distinct neptunyl(V) ions. The $\text{Np}(1)\text{O}_2^+$ and $\text{Np}(2)\text{O}_2^+$, with average Np–O bond lengths of 1.87 and 1.89 Å, are coordinated by five O atoms at the equatorial vertices of pentagonal bipyramids. Np(1) and Np(2) neptunyl bond angles are 171.0(7) and 177.5(8)°, respectively. The bipyramids are distorted, with equatorial Np–O bonds that are as much as 10° from the equatorial plane perpendicular to the NpO_2^+ moiety. The average equatorial bond lengths of Np(1) and Np(2) are 2.46 and 2.47 Å, respectively, consistent with Np(V). $\text{Np}(3)\text{O}_2^+$ has longer bond lengths at 1.96 Å, a bond angle of 176(1)°, and four equatorial O atoms at an average of 2.23 Å that define a square bipyramid. Similarly distorted square bipyramids are known from uranyl structures⁶ and relate to the details of the structural connectivity.

The Np(1) and Np(2) pentagonal bipyramids share an equatorial edge, forming a chain one polyhedron wide with neptunyl ions approximately perpendicular to the chain length. The Np(3) square bipyramid shares two of its edges with adjacent chains of pentagonal bipyramids, linking them into an infinite sheet (Figure 1). This is

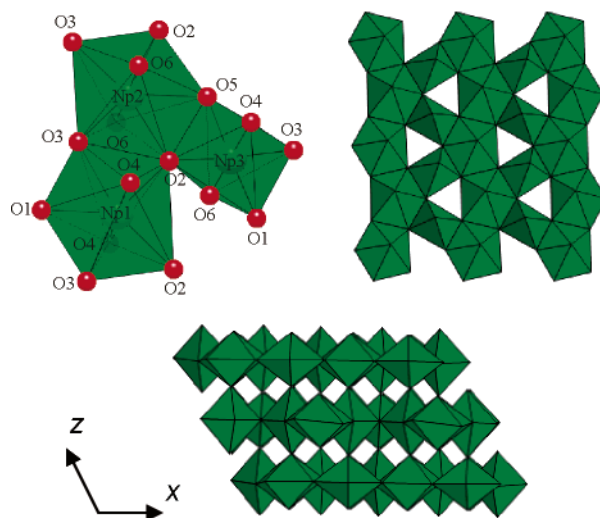


Figure 1. Sheets of square and pentagonal bipyramids in Np_2O_5 (top). Additional linkages between the vertices of the Np(3) square bipyramid and the neptunyl O atoms of the pentagonal bipyramids link the two-dimensional sheet into a three-dimensional framework (bottom).

the first occurrence of such a topological arrangement in a neptunyl compound, although its anions are arranged in the well-known uranophane anion topology that is the basis for the structures of at least 19 uranyl compounds.⁷

The sheet of polyhedra in Np_2O_5 contains “cation–cation interactions” (CCIs), which involve the coordination of the oxo anion of one actinyl moiety as an equatorial ligand of an adjacent actinyl polyhedron.⁸ The $\text{Np}(3)\text{O}_2^+$ donates two CCIs, both of which are accepted by pentagonal bipyramids within the sheet. Put another way, the $\text{Np}(3)\text{O}_2^+$ is oriented approximately parallel with the sheet, and its O atoms are equatorial vertices of Np(1) and Np(2) pentagonal bipyramids. Both O atoms of $\text{Np}(3)\text{O}_2^+$ are equatorial vertices of both the Np(1) and Np(2) bipyramids, and have double CCIs. This connectivity is new in neptunyl compounds but recently was found in a uranyl structure.⁹

Adjacent sheets of polyhedra in Np_2O_5 are linked though CCIs in which the Np(1) and Np(2) neptunyl ion O atoms are equatorial vertices of the Np(3) square bipyramid of an adjacent sheet, and sheets are offset to facilitate this linkage (Figure 1). The orientation of $\text{Np}(3)\text{O}_2^+$ within the sheet facilitates this connectivity.

The details of the CCIs may pertain to the magnetic properties of the structure. Four O atoms of dioxo groups are involved in these interactions. The O(4) and O(6) atoms of the Np(1) and Np(2) neptunyl ions, respectively, link only two neptunyl polyhedra, with Np(1)–O(4)–Np(3) and Np(2)–O(6)–Np(3) bond angles of 174(1) and 169.8(7)°, respectively. In contrast, the O(2) and O(3) atoms, both of the $\text{Np}(3)\text{O}_2^+$ moiety, form double CCIs with Np(3)–O(2)–Np(1), Np(3)–O(2)–Np(2), Np(3)–O(3)–Np(2), and

[†] University of Notre Dame.

[‡] Argonne National Laboratory.

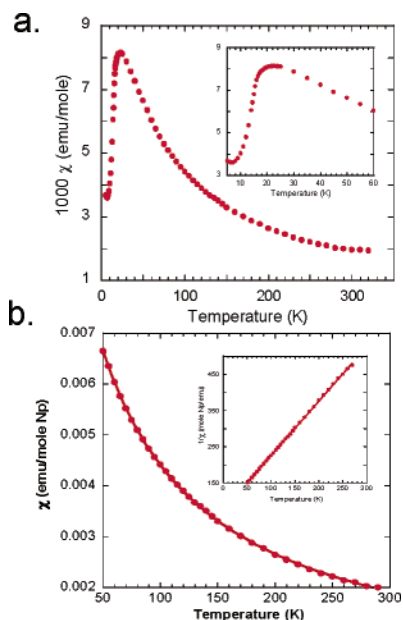


Figure 2. The magnetic susceptibility obtained from 3.8 mg of powdered Np_2O_5 under an applied field of 10000 Gauss. The magnetic susceptibility, plotted as a function of T (a) showing the cusp at 22 K, and (b) above the ordering temperature. The solid line represents the best fit to the data, using a modified Curie–Weiss law. The inset shows the same data, plotted as the inverse susceptibility versus T .

$\text{Np}(3)\text{--O}(3)\text{--Np}(1)$ bond angles of 142(1), 106(1), 143(1), and 104(1) $^\circ$, respectively.

The structure of $\text{K}_2[(\text{UO}_2)_2\text{O}_3]$ contains a sheet of uranyl polyhedra that is topologically identical to that in Np_2O_5 , but the sheets contain no CCIs and are linked through bonds to interlayer K atoms.¹⁰ An early solution of the structure of U_2O_5 ¹¹ provided unrealistic polyhedral geometries and interatomic distances, making it impossible to assess its structural relationship to Np_2O_5 .

$\text{Np}(\text{V})$ has two unpaired spins in an f^2 configuration and, assuming Russell–Saunders coupling, a $^3\text{H}_4$ ground term. Magnetic susceptibility data, from a polycrystalline sample synthesized by the same route as the single crystal, were obtained over the temperature range of 6–300 K (Figure 2). The data reveal a cusp in the magnetic response at 22(3) K, indicating long-range ordering of the moments below that temperature. The falloff of magnetization at lower temperatures is consistent with an antiferromagnetic coupling of the Np moments. Although antiferromagnetism generally dominates ordering in oxide-bridged systems, ferromagnetism dominates neptunyl(V) systems.¹² The ferromagnetic ordering temperatures all appear in the range of about 5–12 K. In contrast, the only example of apparent antiferromagnetic spin ordering occurs in $\text{NaNpO}_2(\text{OH})_2$ at 19.5(5) K.¹³ The broadness of the transition for Np_2O_5 , particularly on the high-temperature side, suggests a relatively complex magnetic structure. Such complex ordering is consistent with the atomic structure that has 3 crystallographically independent NpO_2^+ units, each of which can have a different magnetic moment. In addition, superexchange pathways can be sensitive to both bond lengths and bond angles.¹⁴ The three crystallographic sites have significantly different Np–O–Np superexchange connectivity, with Np–Np interatomic distances ranging from 3.62 to 4.17 Å and Np–O–Np bond angles ranging from 104 to 176.9 $^\circ$. This complexity should generate competing exchange interactions and may account for the broadness in the transition.

Above 50 K the magnetic response is consistent with paramagnetic spins. Figure 2 shows the magnetic response together with a

fit to the data assuming a modified Curie Weiss Law, $\chi_{\text{exp}} = C/(T - \theta) + \chi_{\text{TIP}}$, in which θ , the Weiss constant, is an indication of an interaction energy between local spins, expressed as a temperature and χ_{TIP} is the temperature-independent paramagnetism (TIP). C is the Curie constant and is related to the effective magnetic moment by $\mu_{\text{eff}} = [3kC/(N\mu_B^2)]^{1/2}$ with k as the Boltzmann constant, N as Avogadro's number, and μ_B the units of Bohr magnetons, equal to 0.927×10^{-20} erg/Gauss. The best fit is shown as a line through the data and corresponds to an effective moment of 2.2(1) μ_B , a Weiss constant of $-43(5)$ K, and a TIP of $1.8(8) \times 10^{-4}$ emu/mol Np. The magnitude of the observed effective moment is significantly smaller than the free ion value of 3.58 μ_B expected for an f^2 configuration with Russell–Saunders coupling, as previously observed in two neptunyl(V) sulfate compounds that exhibit ferromagnetic ordering.^{12,15} In contrast, the reduced moment for Np_2O_5 of 2.2(1) μ_B is consistent with those previously observed in paramagnetic¹⁶ and ferromagnetic¹⁷ systems as well as the only other antiferromagnetic material.¹³ Although the reduced moment may be the result of crystal-field effects on the f-spin states,¹⁸ further work is necessary to reveal both the details of the magnetic ordering as well as the electronic details of the Np^{5+} ground state.

Acknowledgment. This work was supported by the Office of Science and Technology and International (OSTI) of the Office of Civilian Radioactive Waste Management (Grant DE-FC28-04RW12255) (ND) and by the U.S. DOE–OBES–Chemical Sciences, under Contract DE-AC02-06CH11357 (ANL).

Supporting Information Available: Complete ref 1, crystallographic CIF file for Np_2O_5 , experimental methods. This material is available free of charge via the Internet at <http://pubs.acs.org>.

References

- (1) Conradson, S. D.; et al. *J. Solid State Chem.* **2005**, *178*, 521–535.
- (2) Haschke, J. M.; Allen, T. H.; Morales, L. A. *Science* **2000**, *287*, 285–287.
- (3) Cohen, D.; Walter, A. J. *J. Am. Chem. Soc.* **1964**, 2696–2699.
- (4) Single crystals of Np_2O_5 were prepared by combining 0.5 mL of 54 mM NpO_2^+ solution with 0.05 g natural calcite crystals followed by heating in a Teflon-lined reaction vessel at 200 $^\circ\text{C}$ for 7 days. The initial and final pH of the solution were 1 and 7.5, respectively. Further details are in Supporting Information.
- (5) Crystallographic data for Np_2O_5 : green crystal of dimensions $75 \times 50 \times 10 \mu\text{m}^3$, monoclinic, $P2_1/c$, $Z = 4$, $a = 8.168(2)$, $b = 6.584(1)$, $c = 9.313(1)$ Å, $\beta = 116.09(1)^\circ$, $V = 449.8(2)$ Å³, $\mu = 45.85 \text{ mm}^{-1}$, $R_1 = 0.0291$, $wR_2 = 0.0635$. Data collection: Bruker SMART APEX II CCD diffractometer, $T = 298$ K, Mo $K\alpha$ $\lambda = 0.71073$ Å, 6578 total reflections, 1665 unique reflections, 904 unique reflections $F_o \geq 4\sigma$. The data were corrected for Lorentz-polarization effects and semiempirically for absorption; the structure was solved by direct methods and refined on the basis of F^2 by full-matrix least squares with 36 parameters.
- (6) Burns, P. C.; Ewing, R. C.; Hawthorne, F. C. *Can. Mineral.* **1997**, *35*, 1551–1570.
- (7) Burns, P. C. *Can. Mineral.* **2005**, *43*, 1839–1894.
- (8) Forbes, T. Z.; Burns, P. C.; Soderholm, L.; Skanthakumar, S. *Mater. Res. Soc. Proc.* **2006**, *893*, 375–380.
- (9) Kubatko, K. A.; Burns, P. C. *Inorg. Chem.* **2006**, *45*, 10277–10281.
- (10) Saine, M. C. *J. Less-Common Met.* **1989**, *154*, 361–365.
- (11) Kovba, L. M.; Komarevtseva, N. I.; Kuzv'mitcheva, E. U. *Radiokhimiya* **1979**, *21*, 754–757.
- (12) Forbes, T. Z.; Burns, P. C.; Soderholm, L.; Skanthakumar, S. *Mater. Res. Soc. Proc.* **2006**, *893*, 375–380.
- (13) Almond, P. M.; Skanthakumar, S.; Soderholm, L.; Burns, P. C. *Chem. Mater.* **2007**, *19*, 280–285.
- (14) Goodenough, J. B. *Magnetism and the Chemical Bond*; Interscience: New York, 1963.
- (15) Forbes, T. Z.; Burns, P. C.; Soderholm, L.; Skanthakumar, S. *Chem. Mater.* **2006**, *18*, 1643–1649.
- (16) Almond, P. M.; Sykora, R. E.; Skanthakumar, S.; Soderholm, L.; Albrecht-Schmitt, T. E. *Inorg. Chem.* **2004**, *43*, 958–63.
- (17) Nakamoto, T.; Nakada, M.; Nakamura, A. *J. Nucl. Sci. Techn.* **2002**, (Suppl. 3), 102–105.
- (18) Staub, U.; Soderholm, L. In *Handbook on the Physics and Chemistry of Rare Earths*; Gschneidner, K. A., Jr., Eyring, L., Maple, M. B., Eds.; Elsevier Science: New York, 1978; Vol. 200030, p 491–545.

JA069250R